

Reservoir Computing for Extraction of Low Amplitude Atrial Activity in Atrial Fibrillation

Andrius Petrėnas¹, Vaidotas Marozas^{1,2}, Leif Sörnmo³, Arūnas Lukoševičius^{1,2}

¹ Biomedical Engineering Institute, Kaunas University of Technology, Kaunas, Lithuania

² Department of Signal Processing, Faculty of Telecommunications and Electronics, Kaunas University of Technology, Kaunas, Lithuania

³ Department of Electrical and Information Technology, Lund University, Lund, Sweden

Abstract

A novel method for QRST cancellation during atrial fibrillation (AF) is introduced for use in recordings with two or more leads. The method is based on an echo state neural network (ESN) which estimates the time-varying, non-linear transfer function between two leads, one lead with atrial activity and another lead without, for the purpose of canceling ventricular activity. The performance is evaluated on ECG signals, with simulated f-waves of low amplitude added, by determining the root mean square error \mathcal{P} between the true f-wave signal and the estimated signal, as well as by evaluating the dominant AF frequency. When compared to average beat subtraction (ABS), being the most widely used method for QRST cancellation, the performance is found to be significantly better with equal to mean and standard deviation of $\bar{\mathcal{P}}_{\text{ESN}} 24.8 \pm 7.3$ and $\bar{\mathcal{P}}_{\text{ABS}} 34.2 \pm 17.9 \mu\text{V}$ ($p < 0.001$). The novel method is particularly well-suited for implementation in mobile health systems where monitoring of AF during extended time periods is of interest.

1. Introduction

The extraction of atrial activity in ECGs recorded during atrial fibrillation (AF) has in recent years received considerable research attention. By canceling the ventricular activity, a connected atrial signal can be produced which is analyzed with respect to f-wave repetition rate and morphology as well as other properties. The development of methods for QRST cancellation has helped to spawn numerous clinical studies in which AF rate (or frequency) is assessed, e.g., for prediction of spontaneous AF behavior and therapeutic effects [1].

The by far most widely used method for QRST cancellation is average beat subtraction (ABS) [2], probably because of its ease of implementation. However, it is well-known that ABS is unable to handle changes in morphol-

ogy as it causes the resulting atrial signal to contain QRST-related residuals. Spatiotemporal QRST cancellation has been proposed for the purpose of handling gradual changes in the electrical axis of the heart, however, this method requires that a multi-lead ECG recording is available [3]. Another group of QRST cancellation techniques explores the assumption that atrial and ventricular activity are generated by different electrical sources so that the surface ECG can be viewed as a linear sum of the sources. Both principal component analysis (PCA) [4] and independent component analysis (ICA) [5] have been proposed to separate signal sources. Crucial issues when using these methods are the identification of the component(s) with atrial activity and the challenge to analyze long-term recordings. Yet another approach to cancel ventricular activity is to employ adaptive Wiener filtering using an Elman artificial neural network [6]. This type of neural network is associated with a slow and complex training process, and its convergence is strongly related to the quality of training data.

Reservoir computing is a recently introduced paradigm in recurrent neural network (RNN) training, of which “echo state networks” (ESNs) are suitable for practical implementation [7]. RNNs have not become popular in applications due to their long and complex training process and potential instability. For ESNs, on the other hand, training is much facilitated by involving only the output connections which are adjusted by simple linear regression. In the present paper, the ESN is proposed as a solution to the problem of QRST cancellation when atrial to ventricular activity ratio is low.

2. Methods

The proposed QRST cancellation method uses a classical adaptive filter approach: the atrial signal is extracted from a mixture of signals using a reference signal which is modified by a filter with time-variable transfer function—the ESN—and an adaptation algorithm, together constitut-

ing the main building blocks of the cancellation, see Fig. 1. The ESN is a large, fixed, recursive neural network which serves as a random nonlinear excitable medium. Its high-dimensional dynamical “echo” response to a driving input is used as a non-orthogonal signal basis to reconstruct the atrial output. The input weights \mathbf{W}_{in} and the reservoir-connecting weights \mathbf{W} are both generated randomly during network initialization from a uniform probability density function (symmetric around zero and invariant to training). The only set of weights which is changed during training is the output weight vector \mathbf{w}_{out} .

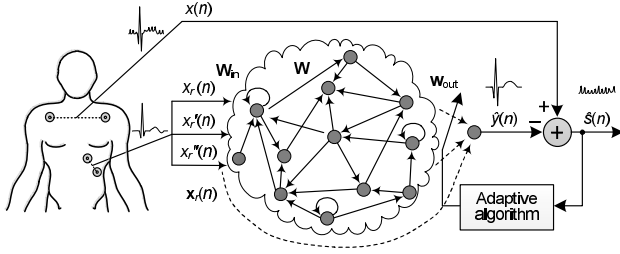


Figure 1. QRST cancellation based on the echo state network. Note that $\hat{y}(n) = g_o(\mathbf{w}_{\text{out}}^T(n-1)\mathbf{z}(n))$.

In this study, the adaptation algorithm of an adaptive filter was employed to train \mathbf{w}_{out} continuously because of rapidly changing QRST morphology. The atrial signal $\hat{s}(n)$ is defined as the error $e(n)$ between the lead subject to cancellation, denoted $x(n)$, and the estimate of the ventricular activity produced by the ESN,

$$\hat{s}(n) \triangleq e(n) = x(n) - g_o(\mathbf{w}_{\text{out}}^T(n-1)\mathbf{z}(n)), \quad (1)$$

where $g_o(\cdot)$ denotes the output neuron activation function and $\mathbf{w}_{\text{out}}(n-1)$ the time-varying output weight vector. The vector $\mathbf{z}(n)$ is the concatenation of the $N \times 1$ reservoir state vector $\mathbf{r}(n)$ and the reference signal $\mathbf{x}_r(n)$, recorded away from the atria,

$$\mathbf{z}(n) = \begin{bmatrix} \mathbf{r}(n) \\ \mathbf{x}_r(n) \end{bmatrix}. \quad (2)$$

The signal $\mathbf{x}_r(n)$ is a vector which includes not only the scalar reference signal $x_r(n)$ but also its first and second derivatives,

$$\mathbf{x}_r(n) = \begin{bmatrix} x_r(n) \\ x_r'(n) \\ x_r''(n) \end{bmatrix}. \quad (3)$$

The inclusion of derivatives offers a more complete characterization of the reference signal, and therefore improves the performance of the ESN. The output weights $\mathbf{w}_{\text{out}}(n)$ of the ESN are updated using the recursive least squares (RLS) algorithm in combination with least squares prewhitening; for details, see [8]. The prewhitening part is

defined by

$$\mathbf{v}(n) = \mathbf{P}(n-1)\mathbf{z}(n), \quad (4)$$

$$\mathbf{u}(n) = \mathbf{P}^T(n-1)\mathbf{v}(n). \quad (5)$$

where $\mathbf{P}(n)$ denotes the inverse of the correlation matrix of $\mathbf{z}(n)$. The update of $\mathbf{P}(n)$ is given by the following two equations:

$$k(n) = \frac{1}{\lambda + \|\mathbf{v}(n)\|^2 + \sqrt{\lambda(\lambda + \|\mathbf{v}(n)\|^2)}}, \quad (6)$$

$$\mathbf{P}(n) = \frac{\mathbf{P}(n-1) - k(n)\mathbf{v}(n)\mathbf{u}^T(n)}{\sqrt{\lambda}}. \quad (7)$$

The forgetting factor λ is a constant which is commonly chosen in the interval $0.95 < \lambda < 1$.

The RLS part of the algorithm produces an update of the output weights,

$$\mathbf{w}_{\text{out}}(n) = \mathbf{w}_{\text{out}}(n-1) + \frac{e(n)\mathbf{u}(n)}{\lambda + \|\mathbf{v}(n)\|^2}. \quad (8)$$

The two parts of the algorithm are initialized by setting

$$\mathbf{w}_{\text{out}}(0) = \mathbf{0}, \quad (9)$$

$$\mathbf{P}(0) = \delta^{-1}\mathbf{I}, \quad (10)$$

where δ is a small positive constant and \mathbf{I} denotes the identity matrix.

The reservoir state vector $\mathbf{r}(n)$ is updated by

$$\mathbf{r}(n) = \alpha\mathbf{r}(n-1) + (1-\alpha)(g_r(\mathbf{W}\mathbf{r}(n-1) + \mathbf{W}_{\text{in}}\mathbf{u}(n))), \quad (11)$$

where the forgetting factor α is a positive constant less than 1, \mathbf{W}_{in} is a $3 \times N$ input weight matrix, \mathbf{W} is an $N \times N$ weight matrix of the internal network connections, $g_r(\cdot)$ a reservoir neuron activation function.

3. Signals and simulations

The proposed method for QRST cancellation is quantitatively evaluated using simulated signals with known f-wave patterns. The f-waves are generated using a sawtooth model, in which both amplitude and repetition rate can be modulated [3]. The model parameter values were chosen similar to those of case A studied in [3], however, in order to produce more challenging signals the model was extended by adding colored noise to $s_d(n)$. Coloring is made through bandpass filtering of white noise (whose variance is a factor 10 smaller than the sawtooth amplitude) with cutoff frequencies at 1.8 and 6.2 Hz. Thus, the f-wave model signal $s(n)$ is composed of a deterministic and a random component:

$$s(n) = s_d(n) + s_r(n). \quad (12)$$

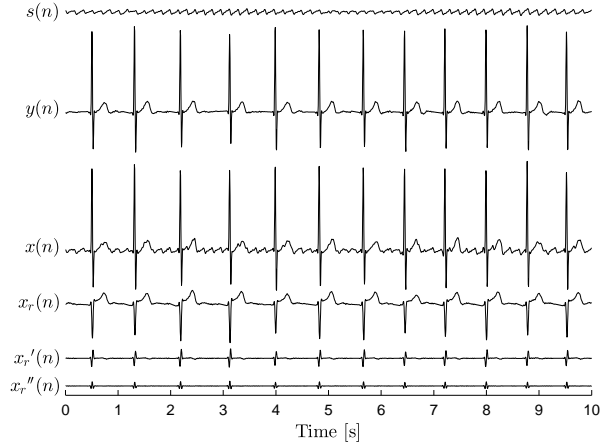


Figure 2. Illustration of a simulated ECG signal: f-wave signal ($\gamma = 30 \mu\text{V}$), ventricular signal (ECG with sinus rhythm but with P waves removed), observed signal, reference signal, and its first and second derivatives.

Seventy-two ectopic-free 1-min segments were selected from two-lead long-term ECG recordings in the MIT-BIH Arrhythmia Database (only segments with normal sinus rhythm) and the MIT-BIH Normal Sinus Rhythm database [9]. The respective sampling rates of the databases were converted to 250 Hz. The output of the f-wave model was then added to one of the two ECG leads, denoted $y(n)$, to produce the signal for analysis:

$$x(n) = y(n) + s(n). \quad (13)$$

The other ECG lead, denoted $x_r(n)$, served as the reference signal. Figure 2 illustrates the atrial, ventricular, and observed signals as well as the reference signal and its derivatives.

In order to reduce the influence of residuals due to misalignment, ABS was performed at an interpolated sampling rate of 1 kHz. It should be noted that ABS was performed only in the lead subject to QRST cancellation, but not in the reference lead.

In this study, the RMS error between $s(n)$ and $\hat{s}(n)$, denoted \mathcal{P} , is the principal performance measure in the time domain. The first second of the analyzed signal was excluded from the computation of \mathcal{P} to avoid the inclusion of transients caused by the cancellation method. The statistical significance of differences in \mathcal{P} is determined using the two-sample t -test. The statistical results are expressed as mean \pm two-sided confidence interval (95%).

Thirty-six of the 72 simulated signals were used for initialization of the ESN parameters, whereas the remaining 36 were used for testing. The “initialization set” contains signals with an f-wave amplitude of $30 \mu\text{V}$. The performance measure \mathcal{P} was computed for each of the 36 simulated signals and then averaged and taken as the overall

performance measure, denoted $\bar{\mathcal{P}}$. Using the initialization set the following parameter values are used for the performance evaluation below: reservoir size $N = 100$, forgetting factors $\lambda = 0.999$, and $\alpha = 0.8$, the reservoir spectral radius set to 1, input scaling set to 1, and reservoir connectivity set to 20%. In addition, the hyperbolic tangent is used as reservoir activation function, whereas the identity activation function is used as output neuron. The RLS algorithm is initialized with $\delta = 0.01$.

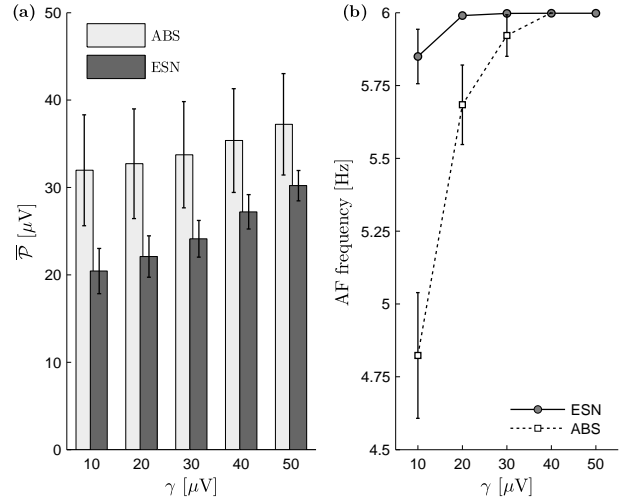


Figure 3. (a) The performance measure $\bar{\mathcal{P}}$ for different f-wave amplitudes using ESN and ABS. (b) Estimates of the dominant AF frequency for a true AF frequency of 6 Hz. Results are expressed as mean \pm two-sided confidence interval.

4. Results

The results presented below are based on the test set with 36 signals, but extended using a fixed f-wave amplitude γ in each set, incremented in steps of $10 \mu\text{V}$ from 10 to $50 \mu\text{V}$. These amplitudes were selected so as to put special emphasis on the problem of how to extract low-amplitude atrial activity, a problem which has not received much attention in the engineering literature.

Figure 3(a) presents the performance of the ESN and ABS in the time domain as quantified by $\bar{\mathcal{P}}$ calculated for the entire signal. The results show that the ESN is much better in extracting the f-wave signal than is ABS with a mean and standard deviation of $\bar{\mathcal{P}}_{\text{ESN}} = 24.8 \pm 7.3$ and $\bar{\mathcal{P}}_{\text{ABS}} = 34.2 \pm 17.9 \mu\text{V}$ ($p < 0.001$). Figure 3(b) displays the results from estimating the dominant AF frequency at different f-wave amplitudes. It is clear that the ESN offers superior performance at most amplitudes: accurate estimates are produced for amplitudes of $20 \mu\text{V}$ or larger, whereas ABS requires at least $40 \mu\text{V}$. The perfor-

mance loss of ABS is largely due to low-frequency residuals of ventricular activity which cause the dominant AF frequency to be underestimated. Figure 4 illustrates the performance of the ESN when ECGs recorded during AF are processed. Lead I and V_1 is subject to cancellation, whereas V_6 is used as the reference lead. Similar to the results obtained on simulated ECG signals, the ESN is capable of handling morphological beat-to-beat variability while ABS struggles when atrial to ventricular activity ratio is low as well as when the single ectopic beat occurs, see Fig. 5.

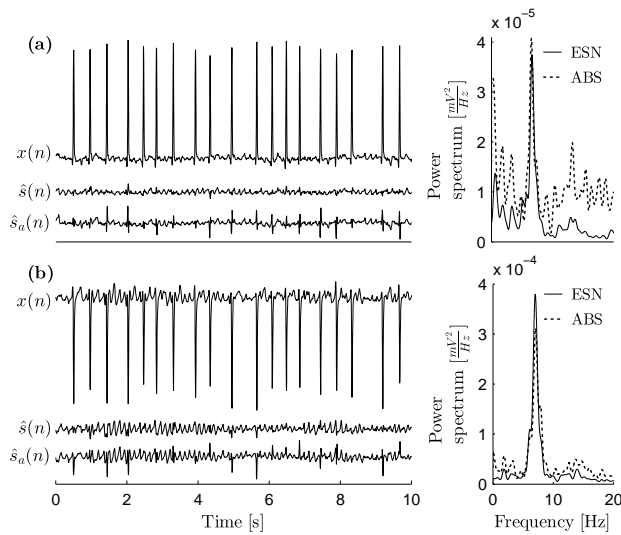


Figure 4. QRST cancellation in ECG signals recorded during AF and corresponding power spectra. The lead subject of cancellation is (a) I and (b) V_1 .

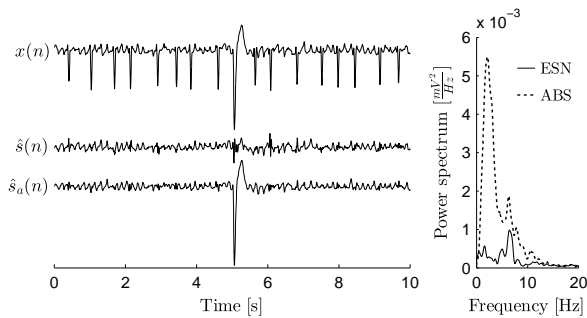


Figure 5. Example of QRST cancellation in ECG signal with single ectopic beat.

5. Conclusions

The present study shows that the ESN is well-suited for cancellation of ventricular activity during AF. Based

on simulated signals as well as ECG examples with AF, the results demonstrate that the handling of small f-waves, variations in beat amplitude and morphology are strengths of the ESN. When comparing performance to that of ABS, the ESN is found to perform better both when quantified in the time and frequency domain. The ESN is suitable for implementation in a system which operates in real time.

Acknowledgements

This work was partially supported by Lithuanian Science Innovation and Technology Agency (project reg. No. 31V-16) and the Swedish Institute (00923/2011).

References

- [1] Bollmann A, Husser D, Mainardi L, Lombardi F, Langley P, Murray A, Rieta JJ, Millet J, Olsson SB, Stridh M, Sörnmo L. Analysis of surface electrocardiograms in atrial fibrillation: Techniques, research, and clinical applications. *Europace* 2006;8:911–926.
- [2] Slocum J, Sahakian AV, Swiryn S. Diagnosis of atrial fibrillation from surface electrocardiograms based on computer-detected atrial activity. *J Electrocardiol* 1992;25:1–8.
- [3] Stridh M, Sörnmo L. Spatiotemporal QRST cancellation techniques for analysis of atrial fibrillation. *IEEE Trans Biomed Eng* 2001;48:105–111.
- [4] Castells F, Mora C, Rieta JJ, Moratal-Pérez D, Millet J. Estimation of atrial fibrillatory wave from single-lead atrial fibrillation electrocardiograms using principal component analysis concepts. *Med Biol Eng Comput* 2005;43:557–560.
- [5] Rieta JJ, Castells F, Sánchez C, Zarzoso V, Millet J. Atrial activity extraction for atrial fibrillation analysis using blind source separation. *IEEE Trans Biomed Eng* 2004;51:1176–1186.
- [6] Vásquez C, Hernández A, Mora F, Carrault G, Passariello G. Atrial activity enhancement by Wiener filtering using an artificial neural network. *IEEE Trans Biomed Eng* 2001;48:940–944.
- [7] Jaeger H. The "echo state" approach to analysing and training recurrent neural networks. GMD Report 148, German National Research Center for Information Technology, 2001.
- [8] Douglas SC. Numerically-robust O(N²) RLS algorithms using least-squares prewhitening. In *IEEE Int. Conf. Acoust., Speech, Signal Proc. (ICASSP)*, volume 25. ISSN 1520-6149, 2000; 412–415.
- [9] Goldberger AL, Amaral LA, Glass L, Hausdorff JM, Ivanov PC, Mark RG, Mietus JE, Moody GB, Peng CK, Stanley HE. PhysioBank, PhysioToolkit, and PhysioNet: Components of a new research resource for complex physiologic signals. *Circulation* 2000;101:E215–220.

Address for correspondence:

Andrius Petrėnas
Studentu st. 65-111, LT-51369, Kaunas
andrius.petrėnas@ktu.lt